Journal of Electronic Imaging 6(4), 439–452 (October 1997).

Nonlinear locally adaptive and iterative algorithms of image restoration

Vladimir P. Melnik
Vladimir V. Lukin
Alexander A. Zelensky
Kharkov Aviation Institute
Department 507, Chkalova Street 17
310070 Kharkov, Ukraine

Heikki Huttunen
Jaakko T. Astola
Tampere University of Technology
Signal Processing Laboratory
P.O. Box 553
FIN-33101, Tampere, Finland
E-mail: hehu@cs.tut.fi

Abstract. *An adaptive approach to restoration of images corrupted by blurring, combined with additive, impulsive and multiplicative noise is proposed. It is based on the combination of nonlinear filters, iterative filtering procedures, and the principles of local adaptation. Numerical simulations and test images illustrating the efficiency of the approach are presented.* © *1997 SPIE and IS&T.*
[S1017-9909(97)00504-7]

1 Introduction

Rather often images are simultaneously corrupted by different types of noise and degraded by blurring. This situation is typical for optical, IR and radiometric imaging.[1–4] The peculiarity of the problem considered in this paper is the assumption that the influence of complex noise, being a combination of additive, impulsive and/or multiplicative noise, is not too high to overwhelm the negative effect of blurring. Therefore, the design of special image restoration procedures aimed at both elimination of blurring and noise reduction are expedient.

There are various approaches to image restoration:[5–8] Wiener and inverse filtering, restoration based on regularization procedures, nonlinear approaches to image recovery, and iterative techniques and algorithms. For the considered situation, for instance, if blurring effects and additive and impulsive noise are present, many restoration methods fail to perform well. In particular, Wiener filtering is unable to remove spikes and it requires reliable information concerning the spectral and statistical properties of the signal and the noise, which is often not available. Inverse filtering sometimes leads to unexpected additional distortions even if the noise level is comparatively low. Regularization procedures can provide a trade-off between noise reduction and blurring removal, but they do not perform well when impulsive noise is present. Nonlinear and iterative methods avoid some drawbacks of the aforementioned techniques, but they are rather complex and require high computational efforts.

The locally adaptive techniques and algorithms of image restoration described by Kuan *et al.*,[3] Zervakis and Katsaggelos,[4] Zervakis and Venetsanopoulos,[9,10] Zervakis and Kwon,[11] and discussed in our papers[12,13] seem to be useful tools for reaching the main goals because they combine the image restoration with adaptive and/or nonlinear filtering.

Here we first demonstrate the efficiency of local adaptation principles[12–14] for image restoration for a traditional image and noise model using the proposed hard-switching procedure and nonlinear filters. Second, we show the steps to take if spikes are present in addition to blurring and additive noise in images. Finally, the results of using the proposed restoration algorithms for images corrupted by multiplicative noise are also presented.

The structure of this paper is the following. Section 2 discusses the peculiarities of well known techniques of image restoration, including those related to the proposed methods and those used for comparison. In Sec. 3 the proposed algorithms are described. The fourth section contains a quantitative analysis of the proposed image restoration procedures and their comparison to well known ones using both quantitative criteria and test images. Finally, conclusions and recommendations are presented.

Paper IST-05 received Jan. 13, 1997; revised manuscript received May 19, 1997; accepted for publication May 29, 1997. This paper is a revision of a paper presented at the SPIE conference on Statistical and Stochastic Methods for Image Processing, Aug. 1996, Denver, CO. The paper pesented there appears (unrefereed) in SPIE Proceedings Vol. 2823.
1017-9909/97/$10.00 © 1997 SPIE and IS&T.

2 Image/Noise Models and Traditional Image Restoration Approaches

As mentioned earlier, usually the images represented as digital (often 8-bit value) two-dimensional (2-D) data arrays are degraded by linear distortions (blurring, defocusing) and corrupted by superposition of additive, impulsive and/or multiplicative and quantization noise. Here we do not discuss the reasons behind these factors because, depending on the situation at hand, they are rather various. Besides, when discussing the properties of the considered restoration algorithms, in some cases the influence of one or two kinds of noise is neglected. In this way it is possible to compare the known and the proposed techniques in situations where they can all be applied.

The generalized model of the sampled image $I(k,l)$ to be reconstructed has the following representation,

$$I(k,l)=u(k,l)\sum_{i,j} h(k-i,l-j)f(i,j)+n(k,l)+d(k,l) +s(k,l), \quad (1)$$

where $k=0,1,\ldots,K-1$ and $l=0,1,\ldots,L-1$ denote the image pixel indices, $K\times L$ is the image size, and $f(k,l)$ defines the ideal image $[f(k,l)\geq 0]$. Furthermore, $h(\Delta k,\Delta l)\geq 0$ denotes the symmetrical defocusing (blurring) function, that is assumed to be spatially invariant. Finally, $u(k,l)$ is the function describing multiplicative noise, $n(k,l)$ is the additive Gaussian white noise, $d(k,l)$ denotes the quantization noise and $s(k,l)$ is the component characterizing impulsive noise. In the following, we have made the following typical assumptions about the noise processes:

$$E[u(k,l)]=1,$$

$$\mathrm{var}[u(k,l)]=\sigma_u^2,$$

$$E[n(k,l)]=0,$$

$$E[n(k,l)n(k+i,l+j)]=0, \text{ if } i\neq 0 \text{ or } j\neq 0,$$

$$\mathrm{var}[n(k,l)]=\sigma_n^2,$$

$$E[d(k,l)]=\Delta/2$$

(or 0 depending on the rounding algorithm),

where Δ is the quantization step equal to unity for the considered 8-bit integer value representation of images. Furthermore, it is assumed that $\mathrm{var}[d(k,l)]=\Delta^2/12$. For simplicity, it is also assumed that $E[u(k,l)u(k+i,l+j)]=0$, $i\neq 0$, $j\neq 0$, i.e., the multiplicative noise is white. Our impulsive noise model is the following: for every image pixel the function $s(k,l)$ has values greater than $3[\sigma_n^2+f^2(k,l)\sigma_u^2]^{1/2}$ with probability P_s, or the value 0 with probability $1-P_s$. In all practical tests, the traditional salt-and-pepper impulsive noise model was used.

In many cases it is expedient to present the model (1) in a vector-matrix form

$$\mathbf{I}=\mathbf{UHf}+\mathbf{n}+\mathbf{d}+\mathbf{s}, \quad (2)$$

where $\mathbf{I}$, $\mathbf{f}$, $\mathbf{n}$, $\mathbf{d}$, and $\mathbf{s}$ are column vectors having dimensions $K\cdot L\times 1$ corresponding to the observed and ideal images, additive, quantization and impulsive noise vectors, respectively. Furthermore, $\mathbf{H}$ and $\mathbf{U}$ denote the blurring function $h(k,l)$ weighting factor Toeplitz matrix and the multiplicative noise diagonal matrix, whose dimensions are $KL\times KL$. The kl'th image sample corresponds to the $(kL+l)$'th element of the vector row if the vector-matrix representation is used.

For solving inverse ill-posed problems of image restoration, the function $h(\Delta k,\Delta l)$ must be known. In some cases, it conforms with the imaging system ambiguity function (called the point-spread function, the directivity pattern or the spatial response). In some situations it can be estimated by using real data or by using *a priori* information about the characteristics of the imaging system and/or the conditions of its operation. Otherwise, some reasonable assumptions or approximations should be used and statistical data can be attracted for this aim.

The classical approach of image restoration concentrates on the situation where

$$\sigma_n^2\neq 0, \quad \sigma_u^2=0, \quad \Delta\ll\sigma_n, \quad P_s=0.$$

Note that the second condition $(\sigma_u^2=0)$ implies that there is no multiplicative noise $[u(k,l)\equiv 1]$. Furthermore, the fourth condition $(P_s=0)$ causes the impulsive-noise term $s(k,l)$ to vanish, and the third condition $(\Delta\ll\sigma_n)$ makes the quantization noise $d(k,l)$ insignificant compared to the Gaussian noise. Under these conditions, the model of Eq. (1) reduces to the classical one

$$I(k,l)=\sum_{i,j} h(k-i,l-j)f(i,j)+n(k,l). \quad (3)$$

This standard situation has been solved and optimal linear filters for this situation are easy to find. Even though the other noise components of the model of Eq. (1) are likely to cause serious problems, the linear filter framework is used as a basis for our approach.

Using the Fourier transform approach one can easily obtain

$$I(\omega_k,\omega_l)=H(\omega_k,\omega_l)F(\omega_k,\omega_l)+N(\omega_k,\omega_l), \quad (4)$$

where $\omega_k=2\pi k/(K-1)$ and $\omega_l=2\pi l/(L-1)$. Furthermore, $I(\omega_k,\omega_l)$, $F(\omega_k,\omega_l)$, $N(\omega_k,\omega_l)$ are the discrete 2-D spatial spectra of $I(k,l)$, $f(k,l)$ and $n(k,l)$, respectively.

In the frequency domain, the inverse filtering is described by the expression

$$\hat{F}(\omega_k,\omega_l)=Y(\omega_k,\omega_l)I(\omega_k,\omega_l)=\frac{1}{H(\omega_k,\omega_l)}I(\omega_k,\omega_l), \quad (5)$$

where $\hat{F}(\omega_k,\omega_l)$ denotes the Fourier transform of the reconstructed image and $Y(\omega_k,\omega_l)=1/H(\omega_k,\omega_l)$ denotes the transfer function of the inverse filter. Note that the in-

fluence of the noise component $N(\omega_k,\omega_l)$ has been neglected. Simultaneously with the distortion (blurring) correction [Eq. (5)] leads to an infinite noise amplification in the high frequency areas. That is why the linear image restoration techniques tend to find a restoration filter $Y(\omega_k,\omega_l)$, which approximates $1/H(\omega_k,\omega_l)$, providing the possibility to correct linear distortions while preventing essential noise amplification. There are several approaches to solving this problem,[15] for example, inverse filtering with a limited bandwidth, or the multiplication of $1/H(\omega_k,\omega_l)$ by some indicator function resulting in the smoothed solution $\hat{F}(\omega_k,\omega_l)$. Another variant is Tikhonov's regularization approach, which uses a stabilizing function $R(\omega_k,\omega_l,\alpha)$:

$$\hat{F}(\omega_k,\omega_l)=\frac{R(\omega_k,\omega_l,\alpha)I(\omega_k,\omega_l)}{H(\omega_k,\omega_l)}, \tag{6}$$

where α is a regularization parameter and $R(\omega_k,\omega_l,\alpha)$ is defined by

$$R(\omega_k,\omega_l,\alpha)=\frac{|H(\omega_k,\omega_l)|^2}{|I(\omega_k,\omega_l)|^2+\alpha\Omega(\omega_k,\omega_l)}. \tag{7}$$

The stabilizing function $\Omega(\omega_k,\omega_l)$ takes into account *a priori* information concerning the ''smoothness'' of an image and the technique described by Eqs. (6) and (7) provides additional noise suppression of high frequency components on the contrary to the inverse filtering [Eq. (5)]. There are some reasons to use the described restoration algorithms. The regularization scheme of Eqs. (6) and (7) results in linear filtering of blurred image. It can be rather easily implemented and requires low computational efforts. Besides, usually it provides appropriate quality of restored image due to the possibility to vary the value α and function $\Omega(\omega_k,\omega_l)$. The simplest regularization function $\Omega(\omega_k,\omega_l)$ can be described by the following expression: $\Omega(\omega_k,\omega_l)=\omega_k^{2t}+\omega_l^{2t}$, where t is the regularization order. Choosing and/or varying α and t it is possible to achieve a trade-off between the blurring correction and the noise smoothing.

The Wiener filter, being optimal with respect to the mean square error (MSE) criterion takes into account the information concerning the image and noise spectral properties [power spatial spectra $S_f(\omega_k,\omega_l)$ and $S_n(\omega_k,\omega_l)$, respectively]. In a generalized form (with parameter α, when it can be termed the controlled Wiener filter) it is described by the following formula

$$R(\omega_k,\omega_l,\alpha)=\frac{|H(\omega_k,\omega_l)|^2}{|I(\omega_k,\omega_l)|^2+\alpha S_n(\omega_k,\omega_l)/S_f(\omega_k,\omega_l)}. \tag{8}$$

This formula obviously requires reliable *a priori* information concerning the spectral characteristics of the imaging system, the image and the noise. Unfortunately, this kind of data are usually not available. Besides, the use of techniques based on optimal estimation theory for image processing often does not provide good results because the criteria used do not match well the psychophysical peculiarities of the human vision. Therefore, even improved techniques of linear restoration[4,15] have a limited applicability. This is also explained by the fact that the assumptions of the noise models behind the theory do not correspond well to practical situations at hand. These aspects relate to all linear image restoration procedures including the Bayesian one.[15]

Nonlinear restoration techniques enable one to eliminate some drawbacks typical of the linear techniques. A class of nonlinear procedures of image restoration is based on a descriptive regularization approach,[16] according to which one must minimize the quality functional[15,16] $\Phi[\mathbf{f}]=\Theta[\mathbf{f}]+C[\mathbf{f},\lambda]+\Omega[\mathbf{f},\alpha]$, which includes $\Theta[\mathbf{f}]$, describing the discrepancy of the ideal image and the obtained solution; a stabilizing functional $\Omega[\mathbf{f},\alpha]$, providing the noise stability of the solution and a restrictions functional $C[\mathbf{f},\lambda]$, containing additional information about the image. These restrictions can be expressed as equations or inequalities, one of which is the required non-negativity of $\mathbf{f}$.

The task of minimizing $\Phi[\mathbf{f}]$ is usually solved by nonlinear programming techniques, thus it requires numerical optimization methods that generally result in significant computational efforts. This is one of the main disadvantages of the nonlinear restoration techniques but the idea of using restrictions is reasonable and prolific.

An alternative method is to use iterative restoration procedures.[6,8] They are relatively simple and enable us to take restrictions into account easily enough. In general, the iterative restoration is described by the following expression

$$F^{m+1}(\omega_k,\omega_l)=I(\omega_k,\omega_l)+[F^m(\omega_k,\omega_l)-H(\omega_k,\omega_l)F^m(\omega_k,\omega_l)], \tag{9}$$

where $m=0,1,2,\ldots$ defines the iteration number for the spatial spectrum domain, and $F^0(\omega_k,\omega_l)\equiv 0$; $F^1(\omega_k,\omega_l)=I(\omega_k,\omega_l)$. In the vector-matrix form one has

$$\mathcal{F}^{m+1}=\mathcal{I}+(\mathbf{1}-\mathcal{H})\mathcal{F}^m, \tag{10}$$

where $\mathcal{F}^0=\mathbf{0}$; $\mathcal{F}^1=\mathbf{I}$, $m=0,1,2,\ldots$ and $\mathbf{1}$ denotes the identity matrix. Here $\mathcal{F}^m$, $\mathcal{I}$, and $\mathcal{H}$ denote the Fourier transforms of the corresponding vectors.

Another advantage of the iterative techniques other than their simplicity is the possibility to use *a priori* restrictions at every iteration. Iterative algorithms with restrictions become nonlinear, which is why they possess the positive features typical of nonlinear restoration methods while preserving the simplicity of the linear restoration techniques. The iterative procedure with restrictions can be described as

$$\mathcal{F}^{m+1}=\mathcal{I}+(\mathbf{1}-\mathcal{H})\Re\mathcal{F}^m, \tag{11}$$

where $\Re$ is the restriction operator (in general it is nonlinear). Typically the restriction operator operates in the spatial domain instead of the spectral domain. It should satisfy the property $\Re\mathcal{F}=\mathcal{F}$, i.e., being applied to the ideal image it must act as an idempotent filter.

The iterative algorithm (9) in the case of no noise converges to the original image; otherwise it is recommended to stop iteration process in order to prevent noise

amplification.[15] The procedure with restrictions of Eq. (11) is more stable to noise influence. Its convergence properties are determined by the restriction operator $\Re$ (Ref. 15).

During the last 10 yr several new adaptive image restoration methods have been proposed.[3,9,10,13] The basic idea behind them is to use different filters for different types of image regions. Practical images usually contain large homogeneous regions and regions with a significant amount of small details, and it is not reasonable to use the same filter for both types. Therefore, the filtering algorithm should pay attention to the type of the region inside the filtering window. Several adaptive algorithms[3,9,10] apply the local mean and the local variance to determine the type of the input sample and to select an appropriate filter. When such algorithms are extended by including the detection of impulses, the resulting algorithms perform well even in complex situations that are described by noise models of Eqs. (1) and (2).

The aforementioned advantages of iterative, nonlinear and locally adaptive restoration procedures stimulated our interest to design adaptive nonlinear iterative algorithms that tend to combine their positive features. Different approaches to the design and application are possible, and in the following some of the most promising ones are presented.

3 Proposed Locally Adaptive Algorithms of Image Restoration

The simplest version of the proposed adaptive image restoration procedure performs a hard-switching[12,13] of the regularization parameter α [see Eqs. (7) and (8)]. The decisions are made according to the comparison of a local adaptation parameter[14] ξ_{kl} with one or several thresholds

$$\hat{\mathbf{f}}_{kl}=\begin{cases}\varphi_{kl}[\mathbf{I},\alpha_1], & \text{if } \xi_{kl}<\xi_1,\\ \varphi_{kl}[\mathbf{I},\alpha_q], & \text{if } \xi_{kl}\in]\xi_{q-1},\xi_q], \quad q=2,\ldots,M,\\ \varphi_{kl}[\mathbf{I},\alpha_M], & \text{if } \xi_{kl}>\xi_M,\end{cases} \tag{12}$$

where $\varphi[\mathbf{I},\alpha_q]$ denotes the result of the filtering of the observed image $\mathbf{I}$ by the restoration procedure of Eq. (7) or Eq. (8) with parameter α_q.

Local adaptation parameter[14] ξ_{kl} indicates the behavior of the original image in the neighborhood of the (k,l)'th pixel. Relatively large values of ξ_{kl} generally correspond to the areas of details. It is known[9,10,15] that in the vicinity of details and edges it is preferable to retain a higher level of noise fluctuations for the sake of resolution enhancement. That is why regularization parameter α should[10,15] be decreased for these regions. Such a recommendation can be realized with the aid of adaptive algorithms. The proposed technique [Eq. (12)] is one of them. It updates α in accordance to the comparison of the adaptation parameter ξ_{kl} to the thresholds.

It is possible to use a soft-switching adaptive image restoration procedure as well, but it is more difficult to implement than the hard-switching procedure. If M is small (for example, 2 or 3) one can acquire $M+1$ images corresponding to different α_q, $q=1,\ldots,M$ by applying the algorithm of fast Fourier transform, performing filtering in the spatial frequency domain and then (after inverse Fourier transformation) selecting the proper value for $\hat{\mathbf{f}}_{kl}$ depending on the results of comparing ξ_{kl} with the thresholds ξ_q.

We have used two typical adaptation parameters that are widely used for data-dependent filtering estimated in the scanning window: the local variance σ_{kl}^2 and the quasirange Q_{kl}, i.e., the difference of the p'th and the r'th order statistics estimated for the sample elements for current scanning window position: $Q_{kl}=I_{kl}^{(p)}-I_{kl}^{(r)}$. Even for small values of M such as $M=1$ or $M=2$ and a proper threshold ξ_q and a parameter α_q, the obtained results for adaptive Wiener and Tikhonov's regularization restoration procedures [the model of Eq. (4)] according to the least MSE (LMSE) criterion outperformed any constant α used for traditional restoration techniques [see Eqs. (7) and (8)] in our tests. The quantitative data are coherent with this conclusion and they are presented in the next section. These successful results stimulated further investigations dealing with more complex and effective image restoration procedures.

The other approach uses locally adaptive robust nonlinear filters as regularizing operators, performing a preliminary smoothing of images. This is stipulated by the fact that the goals of the regularization partially coincide with the aims of locally adaptive robust filtering, i.e., the noise suppression and edge/fine detail preservation. Besides, the locally adaptive nonlinear filters are able to remove impulsive noise and, therefore, to provide the conditions, which the traditional restoration procedures are designed for and applied to. For the considered situation, there are some peculiarities worth noting. First, for blurred images, the edges become ramp and additional blurring that occurs as a consequence of the filtering should be avoided. Furthermore, while removing the spikes, these algorithms should be able to preserve fine details. It is also known that unlike linear filters, nonlinear and adaptive filters in particular can not be described by the spatial frequency characteristics.[17] Thus, their influence on $I(\omega_k,\omega_l)$ can be estimated only approximately. The nonlinear prefiltering changes the statistical and spectral properties of the image and the noise, and the influence of the nonlinear prefilter has to be estimated before further image restoration.

The reasons for their use are the following:

- Adaptive filters characterized by essentially nonlinear properties should be applied only at the first stage of the image processing system, serving the task of impulsive noise removal and that of suppressing other noise components.
- Some important characteristics of this kind of filters valuable for further image restoration can be studied and evaluated using numerical simulation data analysis.

Empirical tests have shown that the best performance was obtained by using the following filters in the preprocessing stage: modified sigma-filter,[18,19] center weighted median (CWM) filter,[20] FIR-median hybrid filters,[21] and adaptive filters[12] based on local variance and the quasirange as the adaptation parameter. According to the comparison of the parameter with the threshold, the use of α-trimmed

mean filtering[17] in the locally passive areas and the use of the modified sigma, CWM or FIR-median hybrid filters in the locally active areas provides the most promising results. The effect of changing the scanning window size and other parameters (for example, the weighting factor of the central pixel for CWM) as a function of the local value of the adaptation parameter were also studied. Some variants are considered in the next section, but the general recommendations are the following. The use of large scanning window sizes (greater than 5×5 pixels) is not reasonable because it can lead to greater distortions in the neighborhood of details and edges. A 5×5 window is usually large enough to provide a reliable impulsive noise removal and an appropriate additive noise suppression efficiency with all reasonable noise quantities.

Finally, the use of the sigma filter as the operator of restrictions is appropriate in some situations. As is known,[19] the standard sigma filter averages only the values belonging to the interval $[I(k,l)-2\sigma_n; I(k,l)+2\sigma_n]$. A modification exists for the case of a dominant influence of multiplicative noise, but both filters are sensitive to spikes. In an earlier paper,[18] we proposed and described the properties of the so-called modified sigma filter as being, in fact, an adaptive filter and possessing better noise suppression efficiency in comparison to the standard sigma filter.[19] Furthermore, our modification enables us to retain the mean level for homogeneous regions of the images and is able to remove spikes. If we suppose that all the noise component variances and P_s are equal to zero, then the sigma filter is an idempotent filter and, thus, the condition $\mathfrak{R}\mathcal{F}=.\mathcal{F}$ of the previous section is satisfied. The same holds approximately for the local statistic Lee filter,[22] but it is unable to remove impulsive noise. This is crucial for the iterative image restoration procedures when the application of nonlinear filtering and linear restoration follow each other. The problem is how to choose the number of iterations and the filtering parameters. The numerical simulations for an 8-bit image have shown that usually performing three iterations is enough and further iterations do not improve the results, essentially because the quantization errors become the dominant factor limiting the possibilities of further image enhancement. It is often reasonable to take some other restrictions into account, in particular, to take care of the positivity of the intermediate and the final solutions as well as to retain the mean level of the reconstructed image.

4 Numerical Simulation Results

To illustrate the proposed methods and to compare them with existing ones, we used the test image "Golden Bridge" shown in Figure 1. It is a good choice for the test image in our case, since it contains a large homogeneous region (the sky), fine details (the bridge and the yacht) and fragments with evident textural features (water surface, hills). Therefore, it is possible to investigate simultaneously different properties of the restoration algorithms: their ability to suppress noise, to preserve texture and to correct blurring effects for edges and fine details. It is also possible to evaluate the corresponding parameters characterizing these properties quantitatively. For the test image, we calculated the following three parameters often used for comparison of efficiency and evaluation of filter properties.[23] Total relative root mean square error (RMSE)

Fig. 1 Original image "Golden Bridge."

$$e_t=\left\{\frac{\Sigma_{k,l}[\hat{f}(k,l)-f(k,l)]^2}{\Sigma_{k,l}[I(k,l)-f(k,l)]^2}\right\}^{1/2}$$

relative RMSE for active and passive areas respectively given by

$$e_a=\left\{\frac{\Sigma_{k,l\in Ap_a}[\hat{f}(k,l)-f(k,l)]^2}{\Sigma_{k,l\in Ap_a}[I(k,l)-f(k,l)]^2}\right\}^{1/2}, \tag{13}$$

$$e_p=\left\{\frac{\Sigma_{k,l\in Ap_p}[\hat{f}(k,l)-f(k,l)]^2}{\Sigma_{k,l\in Ap_p}[I(k,l)-f(k,l)]^2}\right\}^{1/2}, \tag{14}$$

where Ap_a and Ap_p are the sets of pixels classified as belonging to locally active and locally passive image fragments. We detected the edges and details of the original image by calculating the quasirange for every pixel and comparing it to the threshold (see Figure 2 where white pixels indicate the locally active fragments). Joint analysis of these three parameters enables us to investigate the properties of the restoration algorithm from different points of view. The results were also analyzed visually, and the most interesting cases are presented in the figures.

Let us discuss first of all the results for the model Eq. (4). The test image was blurred by a Gaussian function with the width 5 pixels at the level 0.1 and corrupted by independent additive Gaussian noise with variance $\sigma_n^2=7$ (see Figure 3). Table 1 shows the resulting RMSEs for the restoration procedures and filtering algorithms. First, the results for the standard regularization procedure of Eq. (7) are presented for several values of the regularization parameter $\alpha=0.0001$, 0.001, 0.005, 0.05 ($t=3$ in all cases). Obvi-

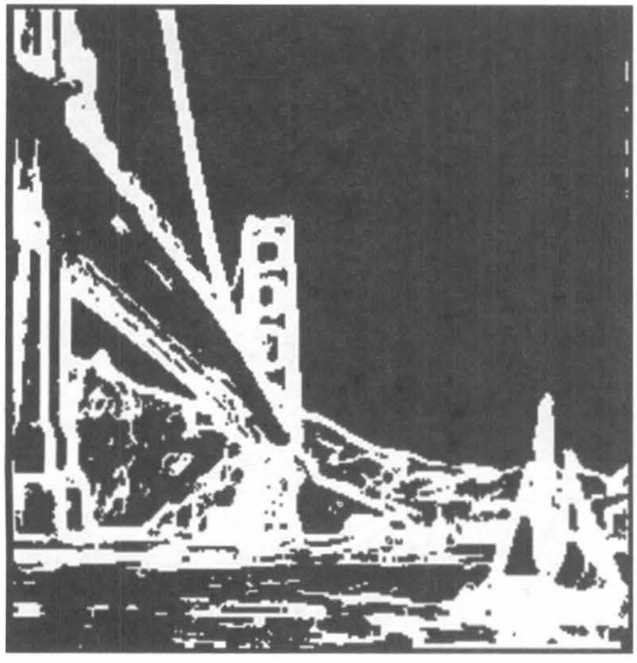

Fig. 2 Locally active and passive regions of the original image (Figure 1).

ously, relatively small values of α result in a better edge/detail restoration (see Figure 4 for $\alpha=0.001$) and the larger values of the parameter α provide better noise suppression for homogeneous regions (see Figure 5 for $\alpha=0.05$). The minimal value of the total RMSE is obtained for value $\alpha=0.001$. The adaptive procedure of Eq. (12), based on the parameter Q_{kl} (with a 5×5 window, $p=18$, $r=8$, $Q_{\text{thresh}}=12$, $M=1$, $\alpha_1=0.05$, $\alpha_2=0.001$) provides a better total RMSE than the standard regularization technique with optimal α. The RMSEs of both the active and the passive regions are close to the best ones among all the tested standard regularization restoration algorithms. The result of the adaptive restoration procedure is shown in Figure 6.

Fig. 3 Distorted image: blurring and additive noise.

Table 1 gives also the results of using the controlled Wiener filter [Eq. (8)] to image restoration. Three values of α were tested: $\alpha=0.5$, 1.0 and 10.0. The adaptive Wiener filter based on the quasirange Q_{kl} (N, p, r and Q_{thresh} are the same as in the previous case) was also studied. Obviously, it also provides improved error correction compared to the standard Wiener filter ($\alpha=1.0$). Figure 7 presents the image reconstructed by the standard Wiener filter and Figure 8 shows the results of the adaptive Wiener restoration. Visual analysis confirms the advantages of the latter approach. Note, however, that for Wiener filtering (including the adaptive version) it is necessary to know the image and noise spectra, but in practice they are usually unknown *a priori*. This is why these results are mainly demonstrative; it is possible to get the spectral information only for test data.

The next four items of Table 1 reflect the properties of the use of preliminary filtering and further regularization ($t=3$, $\alpha=0.0001$) to processing the test image. Four filtering algorithms were studied: the CWM filter with the weight w of the central pixel equal to three and the cross 3×3 window. The next two cases show the results of using the sigma filter with window sizes 5×5 and 3×3 as the prefilter. Finally, the last case considers the use of their adaptive combination as the prefilter. The adaptive filter determines the type of the region inside the filter window by calculating the quasirange ($p=18$, $r=8$) inside the 5×5 square window and comparing it with the threshold $Q_{\text{thresh}}=12$. In locally passive regions, the image was filtered by the sigma filter with a 5×5 square window, and in locally active regions the filtering is done by the CWM using a 3×3 cross-shaped window with center weight equal to three. The resulting image of the last algorithm is presented in Figure 10. Comparing the obtained quantitative and visual results of the image processing techniques for regularization restoration (first item of Table 1 and Figure 9), it is seen that the preliminary filtering is expedient. It provides noise suppression for locally passive regions and after this the restoration based on regularization corrects the blurring well due to a small value of α.

Finally, the iterative image restoration procedures of Eq. (11) with and without the use of nonlinear filters as the operator of restrictions were analyzed. For practical reasons the pixel values of the reconstructed image were truncated to integers after every iteration. Table 2 contains the results for several variants of the algorithm, with different number of iterations. The first is the standard iterative restoration procedure [Eqs. (9) and (10)] (see Figure 11).

The other items of Table 2 compare the CWM filter, the sigma filter and an adaptive filter. The CWM filter used a 3×3 cross-shaped window with central pixel weight equal to 3. The tests with the sigma-filter were done with a 5×5 square window. In the adaptive filtering, the sigma filter was used for the locally passive fragments and the CWM filter for locally active fragments. The quasirange was used as the adaptation parameter, and it was estimated using the 5×5 square window ($p=18$, $r=8$, $Q_{\text{thresh}}=12$). Figure 12 shows the result of using the adaptive filter as the

Table 1 Quantitative results of reconstruction with different parameters.

Item	Parameters of Reconstruction		Relative RMSE		
	Restoration Algorithm	Preliminary Filter	e_t	e_a	e_p
1	Regularization, $\alpha=0.0001$, $t=3$	—	1.110	0.792	1.870
2	Regularization, $\alpha=0.001$, $t=3$	—	0.870	0.783	1.160
3	Regularization, $\alpha=0.005$, $t=3$	—	0.900	0.870	0.990
4	Regularization, $\alpha=0.05$, $t=3$	—	1.010	1.030	0.950
5	Adaptive regularization[1]	—	0.824	0.787	0.950
6	Wiener filter, $\alpha=10$	—	0.926	0.926	0.919
7	Wiener filter, $\alpha=1.0$	—	0.802	0.717	1.060
8	Wiener filter, $\alpha=0.5$	—	0.828	0.687	1.220
9	Adaptive Wiener filter[2]	—	0.740	0.689	0.920
10	Regularization, $\alpha=0.0001$, $t=3$	CWM, cross 3×3	0.974	0.770	1.500
11	Regularization, $\alpha=0.0001$, $t=3$	Sigma, 5×5 square	0.873	0.783	1.150
12	Regularization, $\alpha=0.0001$, $t=3$	Sigma, 3×3 square	0.910	0.787	1.267
13	Regularization, $\alpha=0.0001$, $t=3$	Adaptive filter[3]	0.862	0.767	1.148

[1]Quasirange was used as the adaptation parameter (5×5 window, $p=18$, $r=8$, $Q_{\text{thresh}}=12$), $M=1$, $t=3$, $\alpha_1=0.05$, $\alpha_2=0.001$.

[2]Quasirange was used as the adaptation parameter (5×5 window, $p=18$, $r=8$, $Q_{\text{thresh}}=12$), $M=1$, $\alpha_1=10$, $\alpha_2=0.5$.

[3]Quasirange was used as the adaptation parameter (5×5 window, $p=18$, $r=8$, $Q_{\text{thresh}}=12$), sigma filter, square 5×5 window+CWM, cross 3×3 window, $w=3$.

preliminary filter and as the restriction operator.

From Table 2 one can see that the more complex is image processing procedure used, the better is the quality of the resulting image compared to the standard linear techniques described by Eqs. (7), (8), (9), and (10). When the adaptive filter is used both as a prefilter and as the operator of restrictions, the resulting RMSE is the smallest. However, increasing the number of iterations beyond three does not increase the performance of the filtering algorithm.

Note that the goal of the prefilter is to suppress the external noise essentially while preserving the information contained in the blurred image. On the other hand, the operator of restrictions is used to avoid fluctuations caused by the amplification of the high-frequency components during the reconstruction. Thus, the prefilter has to be less detail-preserving than the one used as the operator of restrictions.

Let us now demonstrate the efficiency of the proposed reconstruction procedures for other noise models. The first

Fig. 4 Result of restoration by regularization, $\alpha=0.001$.

Fig. 5 Result of restoration by the regularization method, $\alpha=0.05$.

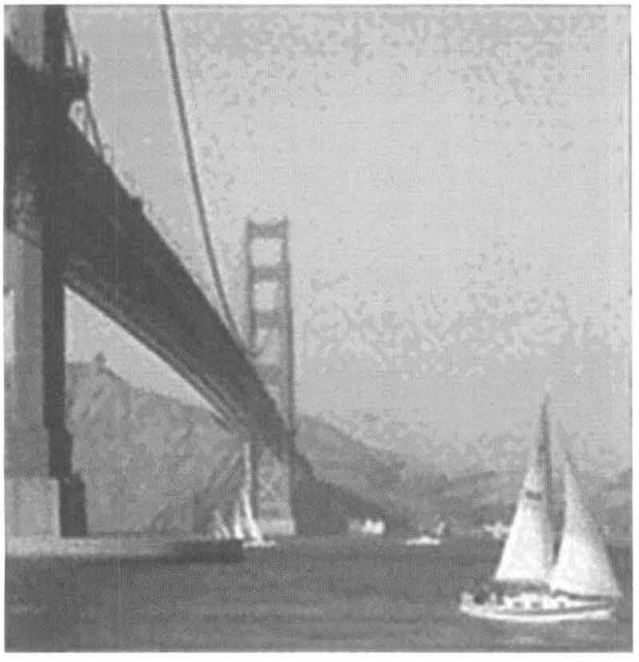

Fig. 6 Result of the adaptive regularization method.

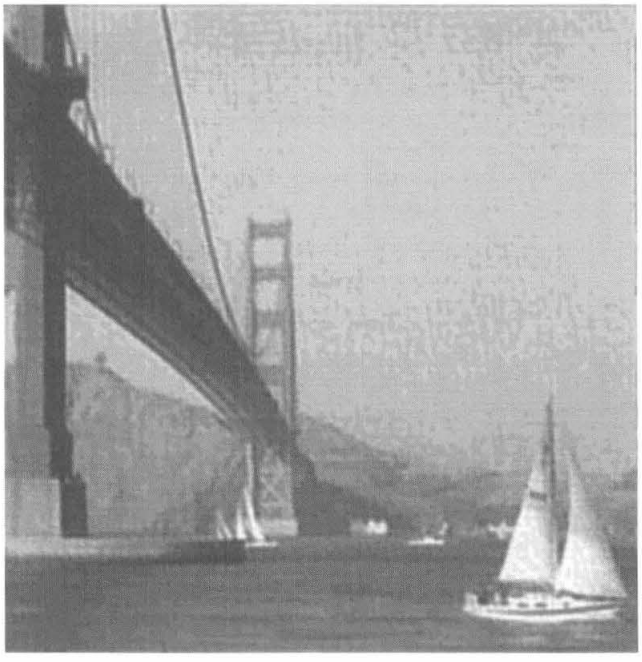

Fig. 8 Results of filtering the distorted image (Fig. 3) by the adaptive Wiener filter.

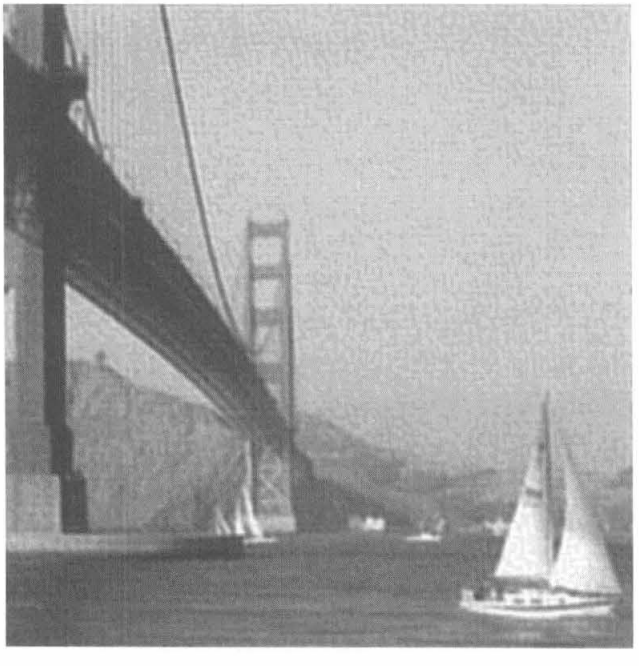

Fig. 7 Results of filtering the distorted image (Fig. 3) by the Wiener filter.

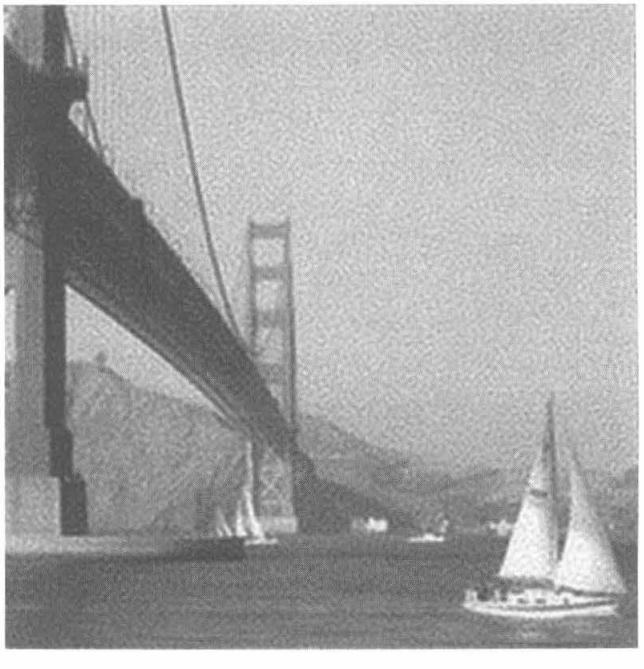

Fig. 9 Results of filtering the distorted image (Fig. 3) by the regularization method, $\alpha = 0.0001$.

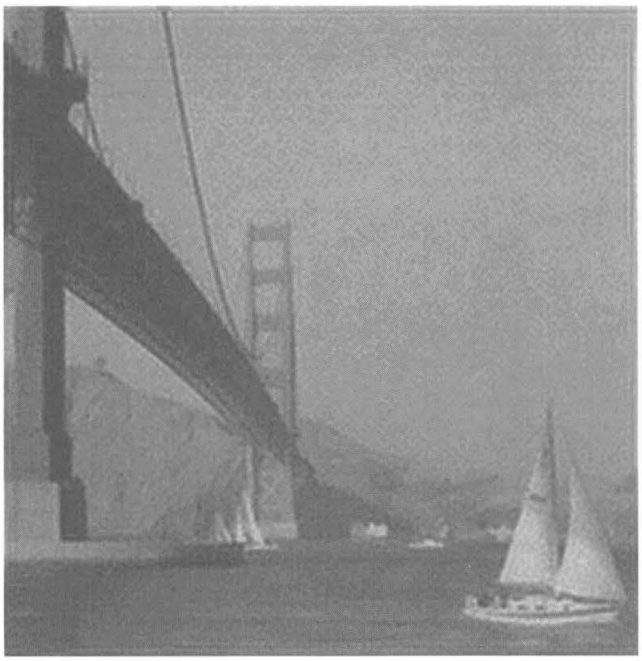

Fig. 10 Results of filtering the distorted image (Fig. 3) by adaptive preliminary filtering and the regularization method, $\alpha = 0.0001$.

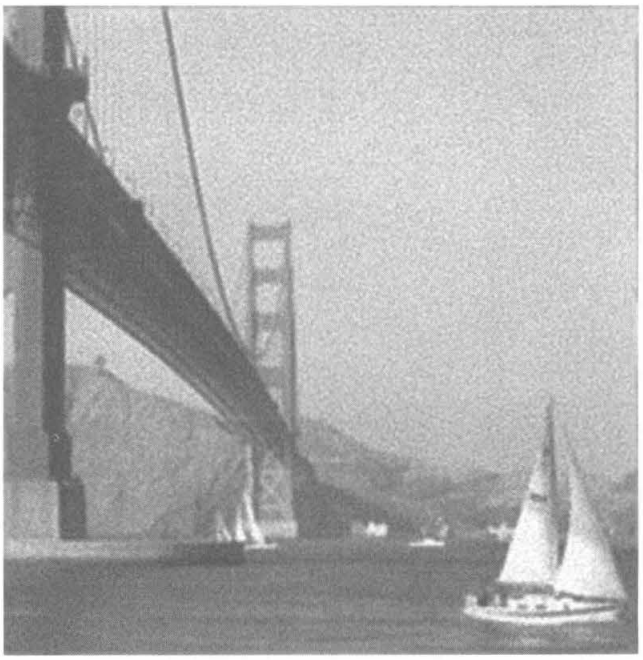

Fig. 11 Results of filtering the distorted image (Fig. 3) by the standard iterative procedure.

case is the superposition of additive and impulsive noise ($\sigma_n^2 = 7$, $P_s = 0.01$). The corresponding blurred image is shown in Figure 13. The numerical results are shown in Table 3. The first row shows the results for the regularization procedure with parameters $t = 3$ and $\alpha = 0.001$. From Figure 14 one can obviously see that this method fails when spikes are present. We have analyzed the use of some robust nonlinear filters for preliminary processing of images before reconstruction using regularization. The tested filters are the CWM with the 3×3 cross window and center weight $w = 3$, the standard median with the 3×3 square window and their adaptive combination based on the calculation of the quasirange and its comparison with a predetermined threshold. The latter variant gives the best result, which can be clearly seen from the fourth row of Table 3, and also from Figure 15, which compared with Figure 14, contains no such artifacts that are produced during the regularization.

The second part of Table 3 contains the empirical data of the reconstruction by the iterative algorithm in the presence of additive noise and spikes. The tests were performed with different numbers of iterations and with different filters for the prefiltering and for the restriction operator. Figure 16 presents the resulting image for a simple iterative procedure, where the number of iterations is three. It can be observed that the spikes remain and degrade the image quality significantly. This can, however, be avoided by using preliminary filtering and an operator of restrictions. The results of using such an operator are shown in row 12 of Table 3 and Figure 17. Obviously, the spikes are removed and the image is enhanced essentially. From the results

Table 2 Quantitative results of iterative reconstruction with additive noise.

	Parameters of Reconstruction		One Iteration			Three Iterations			Five Iterations		
Item	Preliminary Filter	Restriction Operator	e_t	e_a	e_p	e_t	e_a	e_p	e_t	e_a	e_p
1	—	—	0.970	0.856	1.326	1.240	0.881	2.097	1.540	1.026	2.844
2	CWM, 3×3 cross, $w = 3$	—	0.900	0.855	1.080	1.020	0.850	1.480	1.220	0.963	1.890
3	—	CWM, 3×3 cross, $w = 3$	0.930	0.852	1.180	1.010	0.819	1.540	1.150	0.866	1.860
4	CWM, 3×3 cross, $w = 3$	CWM, 3×3 cross, $w = 3$	0.910	0.855	1.085	0.970	0.816	1.400	1.080	0.854	1.680
5	Sigma, 5×5 square	—	0.880	0.854	0.980	0.960	0.975	1.240	1.140	1.010	1.550
6	Sigma, 5×5 square	CWM, 3×3 cross, $w = 3$	0.873	0.854	0.940	0.872	0.826	1.024	0.970	0.872	1.110
7	Adaptive filter[1]	—	0.880	0.855	0.980	0.950	0.851	1.240	1.110	0.970	1.550
8	Adaptive filter[1]	Adaptive filter[1]	0.880	0.857	0.960	0.850	0.814	0.971	0.890	0.852	1.030

[1]Quasirange was used as the adaptation parameter (5×5 square window, $p = 18$, $r = 8$, $Q_{\text{thresh}} = 12$). Sigma filter with a square 5×5 window was used in the passive areas and the CWM filter with a 3×3 cross window and central weight $w = 3$ was used in the active areas.

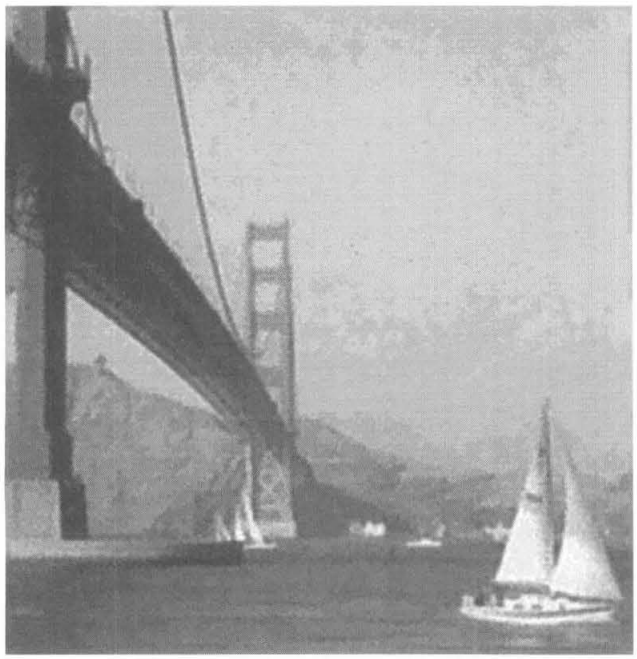

Fig. 12 Results of filtering the distorted image (Fig. 3) by an iterative procedure where an adaptive filter was used as the preliminary filter and as the restriction operator.

Fig. 13 Distorted image: blurring, additive and impulsive noise.

concerning the reconstruction by the iterative algorithm, it can be concluded that the use of both the preliminary image filtering and the operator of restrictions is expedient. In addition to that, the computational load does not become too extensive, because only a small number of iteration steps are needed for good results.

We also studied the case of simultaneous influence of blurring and multiplicative noise with variance $\sigma_u^2 = 0.0025$. The initial blurred and noisy image is presented in Figure 18. The application of reconstruction techniques to this situation has no definite theoretical background, but as shown by results of Kuan and Zervakis, it is nevertheless expedient. Certainly, in the considered situation the modification of filtering algorithms applicable to multiplicative noise suppression should be used. The numerical simulation data for different noniterative (preliminary nonlinear filtering+regularization) and iterative (different combinations of preliminary filtering and/or restriction operators) methods are presented in Table 4, which shows that practically in all cases the use of the modified sigma filter[18] provides the best results. Concerning iteration number, the recommendations are similar to those for the previous cases. The result of preliminary image filtering by means of the sigma filter with the square 5×5 window and further

Table 3 Quantitative results of reconstruction for additive noise and spikes.

	Parameters of Reconstruction			Relative RMSE		
Item	Restoration Algorithm	Preliminary Filter	Restriction Operator	e_t	e_a	e_p
1	Regularization, $\alpha=0.001$, $t=3$	—	—	1.400	1.190	1.540
2	Regularization, $\alpha=0.001$, $t=3$	CWM, 3×3 cross, $w=3$	—	0.550	0.678	0.426
3	Regularization, $\alpha=0.001$, $t=3$	Median: 3×3 square	—	0.564	0.752	0.356
4	Regularization, $\alpha=0.001$, $t=3$	Adaptive filter[1]	—	0.524	0.679	0.361
5	Iterative algorithm, one step	—	—	1.018	0.924	1.085
6	Iterative algorithm, three step	—	—	1.166	0.976	1.293
7	Iterative algorithm, five steps	—	—	1.343	1.090	1.510
8	Iterative algorithm, one step	CWM, 3×3 cross, $w=3$	—	0.581	0.737	0.423
9	Iterative algorithm, three steps	CWM, 3×3 cross, $w=3$	—	0.624	0.713	0.546
10	Iterative algorithm, five steps	CWM, 3×3 cross, $w=3$	—	0.694	0.746	0.651
11	Iterative algorithm, one step	Adaptive filter[1]	Adaptive filter[1]	0.553	0.738	0.349
12	Iterative algorithm, three steps	Adaptive filter[1]	Adaptive filter[1]	0.536	0.707	0.353
13	Iterative algorithm, five steps	Adaptive filter[1]	Adaptive filter[1]	0.553	0.733	0.356

[1]Median: 3×3 square in the passive and CWM with 3×3 cross and central weight $w=3$ in the active areas.

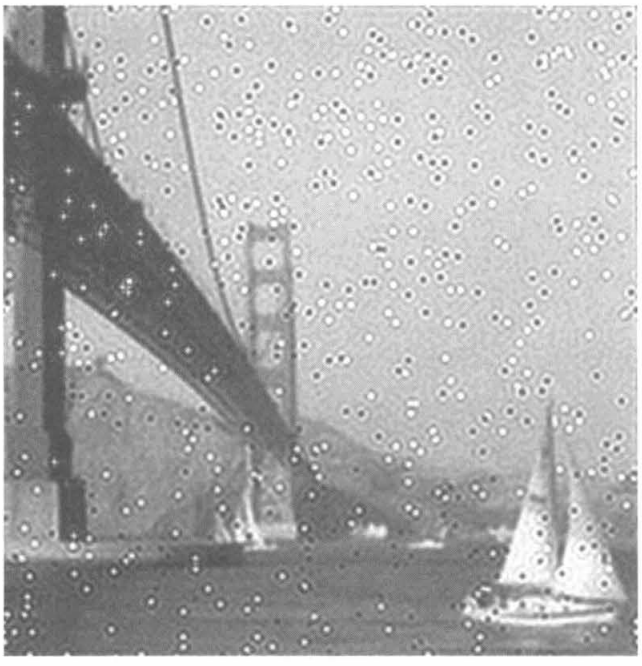

Fig. 14 Results of filtering the distorted image (Fig. 13) by the regularization algorithm, $\alpha = 0.001$.

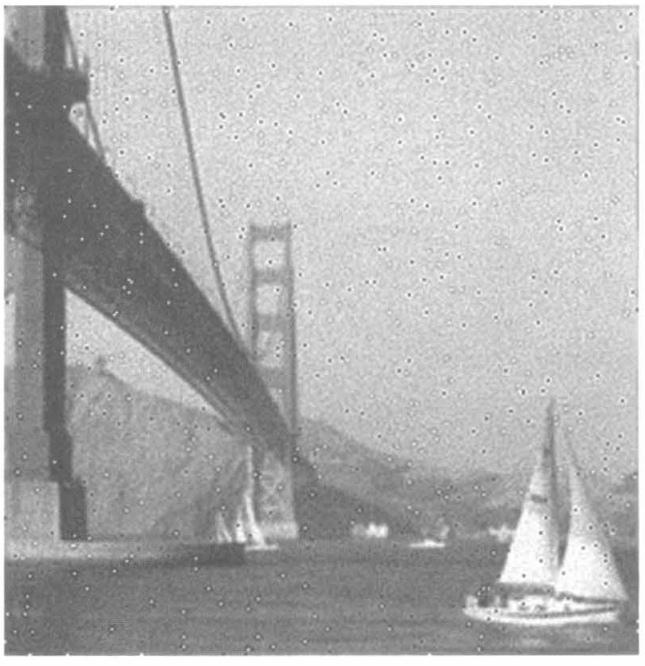

Fig. 16 Results of filtering the distorted image (Fig. 13) by a simple iterative procedure.

Fig. 15 Results of restoring the distorted image (Fig. 13) by preliminary filtering by an adaptive filter and the regularization method, $\alpha = 0.001$.

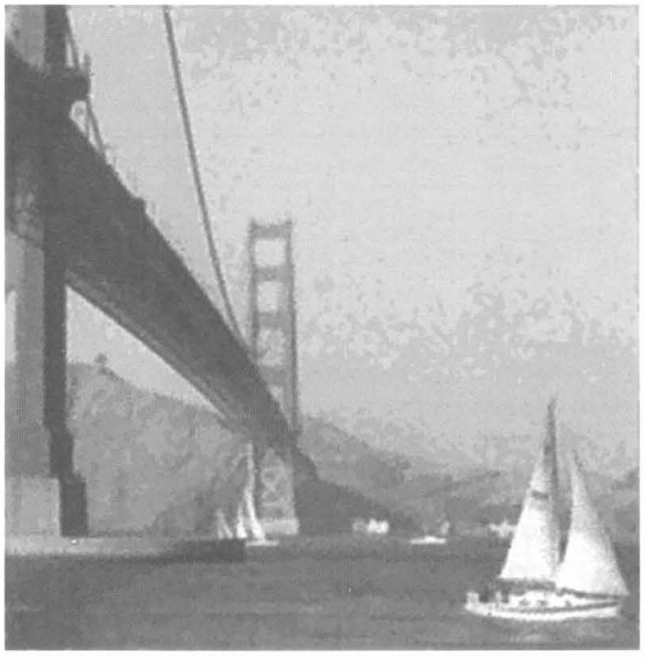

Fig. 17 Results of restoring the distorted image (Fig. 13) by an iterative procedure, where an adaptive filter is used as the preliminary filter and as the restriction operator.

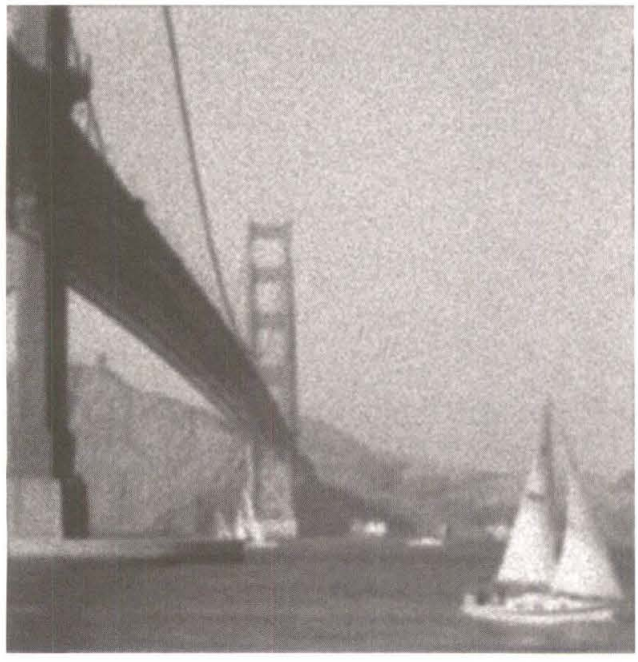

Fig. 18 Distorted image: blurring and multiplicative noise.

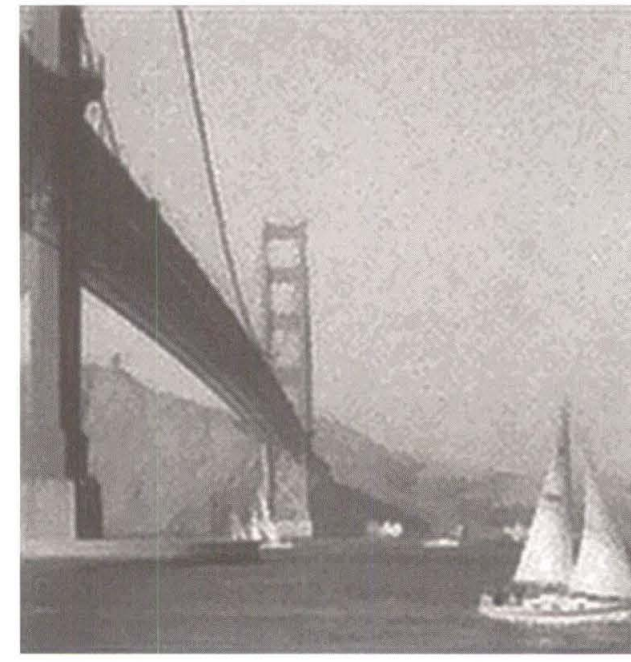

Fig. 19 Results of restoring the distorted image (Fig. 18) by preliminary filtering by the sigma filter and the regularization method, $\alpha = 0.001$.

regularization reconstruction ($\alpha = 0.001$, $t = 3$) is represented in Figure 19. The use of another scheme (item 11) is demonstrated by Figure 20. The image is obtained using a preliminary modified sigma filter having a 5×5 square window that is also used as the restriction operator for iterative (three iterations) reconstruction. The edge preservation is almost equal, but the noise suppression efficiency at the homogeneous regions is worse.

5 Conclusions

The obtained results show that the image restoration techniques, combined with the local adaptation approach and the use of a nonlinear filter as preliminary processing algorithms and/or the operator of restrictions for iterative procedures, are able to provide the enhancement of images simultaneously distorted by blurring effects and corrupted by superposition of different kinds of noises: additive, multiplicative and impulsive. The recommendations concerning nonlinear filter type and parameter selection were presented and the goals of every processing algorithm were discussed. Quantitative data confirms the efficiency of the proposed procedures.

Table 4 Quantitative results of reconstruction for multiplicative noise.

	Parameters of Reconstruction			Relative RMSE		
Item	Restoration Algorithm	Preliminary Filter	Restriction Operator	e_t	e_a	e_p
1	Regularization, $\alpha = 0.001$, $t = 3$	—	—	1.064	0.858	1.335
2	Regularization, $\alpha = 0.001$, $t = 3$	CWM, 3×3 cross, $w = 3$	—	0.981	0.846	1.160
3	Regularization, $\alpha = 0.001$, $t = 3$	Median: 3×3 cross	—	0.880	0.846	0.932
4	Regularization, $\alpha = 0.001$, $t = 3$	Local statistic, Lee 3×3 square window	—	0.839	1.090	0.945
5	Regularization, $\alpha = 0.001$, $t = 3$	Sigma, 5×5 square, 3×3 square window	—	0.790	0.822	0.737
6	Iterative algorithm, one step	—	—	1.280	0.964	1.658
7	Iterative algorithm, three steps	—	—	2.067	1.247	2.919
8	Iterative algorithm, five steps	—	—	2.842	1.621	4.075
9	Iterative algorithm, one step	Sigma, 5×5 square	Sigma, 5×5 square	0.832	0.914	0.683
10	Iterative algorithm, three steps	Sigma, 5×5 square	Sigma, 5×5 square	0.895	0.983	0.737
11	Iterative algorithm, five steps	Sigma, 5×5 square	Sigma, 5×5 square	1.002	1.109	0.807
12	Iterative algorithm, one step	Sigma, 5×5 square	Sigma, 3×3 square	0.828	0.908	0.684
13	Iterative algorithm, three steps	Sigma, 5×5 square	Sigma, 3×3 square	0.893	0.974	0.750
14	Iterative algorithm, five steps	Sigma, 5×5 square	Sigma, 3×3 square	1.010	1.106	0.837

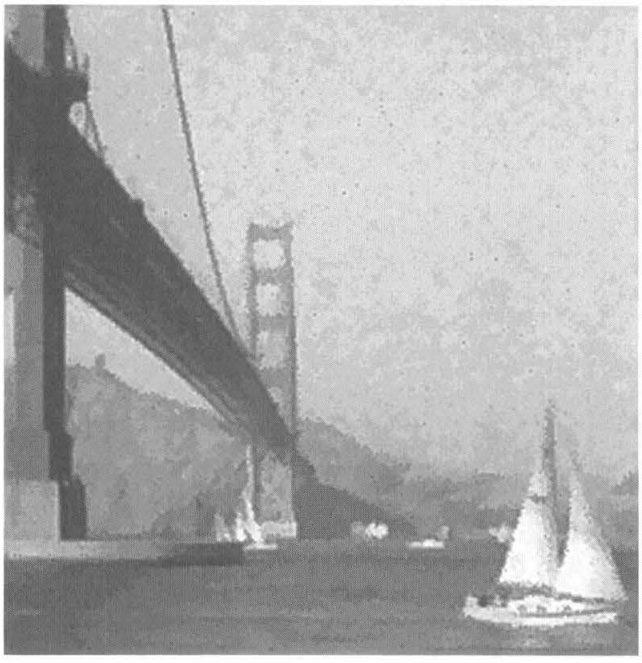

Fig. 20 Results of restoring the distorted image (Fig. 18) by an iterative procedure where the sigma filter is used as the preliminary filter and as the restriction operator.

Similar results were obtained for other variances of additive and multiplicative noise and different degrees of image blurring. The proposed algorithms seem to be more simple than the robust image reconstruction ones put forward by Katsaggelos, Zervakis and Kwon. Comparing our approach to that described by Zervakis and Venetsanopoulos we emphasize that some ideas are similar but we used other filters characterized by better detail preservation properties and the Q-parameter for locally active area detection (for adaptive filters), which is robust with respect to spikes.

References

1. S. Geman and D. Geman, "Stochastic relaxation, Gibbs distributions, and the Bayesian restoration of images," *IEEE Trans. Pattern Anal. Mach. Intell.* **PAMI-6**(6), (1984).
2. S. A. Kassam and H. V. Poor, "Robust techniques for signal processing: a survey," *Proc. IEEE* **PROC-73**(3), 433–481 (1985).
3. D. T. Kuan, A. A. Sawchuk, T. C. Strand, and P. Chavel, "Adaptive restoration of images with speckles," *IEEE Trans. Acoust. Speech Signal Process.* **ASSP-35**, 373–383 (1987).
4. M. E. Zervakis and A. K. Katsaggelos, "A class of robust entropic functionals for image restoration," *IEEE Trans. Image Process.* **4**, 752–773 (June 1995).
5. H. C. Andrews and B. R. Hunt, *Digital Image Restoration*, Prentice-Hall, Englewood Cliffs, NJ (1977).
6. A. K. Katsaggelos, Ed., *Digital Image Restoration*, Springer Series in Information Sciences, Vol. 23, Springer-Verlag, Berlin, Vienna, New York (1991).
7. A. K. Katsaggelos, "Iterative image restoration algorithms," *Opt. Eng.* **28**(7), 735–748 (1989).
8. A. K. Katsaggelos, J. Biemond, R. W. Schafer, and R. M. Mersereau, "A regularized iterative image restoration algorithm," *IEEE Trans. Signal Process.* **SP-39**, 914–929 (Apr. 1991).
9. M. E. Zervakis and A. N. Venetsanopoulos, "Linear and nonlinear image restoration under the presence of mixed noise," *IEEE Trans. Circ. Syst.* **CAS-38**, 258–272 (1991).
10. M. E. Zervakis and A. N. Venetsanopoulos, "A class of noniterative estimators for nonlinear image restoration," *IEEE Trans. Circ. Syst.* **CAS-38,** 731–744 (1991).
11. M. E. Zervakis and T. M. Kwon, "Robust estimation techniques in regularized image restoration," *Opt. Eng.* **31**(10), 2174–2190 (1992).
12. V. V. Lukin, A. A. Kurekin, V. P. Melnik, and A. A. Zelensky, "Application of order statistic filtering to multichannel radar image processing," in *Symp. on Electronic Imaging: Science and Technology, Proc. IS&T/SPIE* **2224A**, 302–312 (1995).
13. V. P. Melnik, "Locally-adaptive algorithms of image restoration," in *Proc. 2nd All-Ukrainian Int. Conf. on Signal/Image Processing and Pattern Recognition*, pp. 211–214, Kiev, Ukraine (1994).
14. V. V. Lukin, V. P. Melnik, A. B. Pogrebniak, A. A. Zelensky, J. T. Astola, and K. P. Saarinen, "Digital adaptive robust algorithms for radar image filtering," *J. Electron. Imaging* **5**(3), 410–421 (1996).
15. G. I. Vasilenko and A. M. Taratorin, *Image Reconstruction*, Radio i swjaz, Moscow (1986) (in Russian).
16. S. E. Falkovich, V. I. Ponomarev, Y. V. Shkvarko, *Optimal Reception of Spatial-Temporal Signals in Radio Channels with Dispersion*, Radio i swjaz, Moscow (1989) (in Russian).
17. I. Pitas and A. N. Venetsanopoulos, *Nonlinear Digital Filters: Principles and Applications*, Kluwer Academic, Boston (1990).
18. V. Lukin, N. N. Ponomarenko, P. Kuosmanen, and J. Astola, "Modified sigma filter for processing of images corrupted by multiplicative and impulsive noises," in *Proc. of EUSIPCO-96*, Vol. III, pp. 1909–1912, Trieste, Italy (Sep. 1996).
19. J.-S. Lee, "Digital image smoothing and the sigma filter," *Comput. Vis. Graph. Image Process.* **24**, (1983).
20. J. Ko and J.-H. Lee, "Center weighted median filters and their application to image enhancement," *IEEE Trans. Circ. Syst.* **CAS-38**, 984–993 (1991).
21. A. Nieminen, P. Heinonen, and Y. Neuvo, "A new class of detail preserving filters for image processing," *IEEE Trans. Pattern Anal. Mach. Intell.* **PAMI-9**, 74–90 (1987).
22. J.-S. Lee, "Digital image enhancement and noise filtering by use of local statistics," *IEEE Trans. Pattern Anal. Mach. Intell.* **PAMI-2**, 165–168 (1980).
23. J. M. H. du Buf and T. G. Campbell, "A quantitative comparison of edge-preserving smoothing techniques," *Sign. Proc.* **21**, 289–301 (Dec. 1990).

Vladimir P. Melnik graduated from the Kharkov Aviation Institute, Faculty of Radioengineering Systems, in 1992 and received his PhD in radioengineering in 1996. Currently he is a senior research fellow at the Kharkov Aviation Institute. His research area is adaptive nonlinear filtering and restoration.

Vladimir V. Lukin graduated from the Kharkov Aviation Institute, Faculty of Radioengineering Systems, in 1983 and received his PhD in radioengineering in 1988. He was a junior researcher and then a senior researcher with the Department of Transmitting and Receiving Devices of Kharkov Aviation Institute. From 1992 to 1993 he was a visiting scholar in the Northern Jiaotong University, Beijing, China. Currently he is a department vice chairman at the Kharkov Aviation Institute. His research area is adaptive nonlinear signal and image processing.

Alexander A. Zelensky graduated in 1966 from the Kharkov Aviation Institute, Faculty of Radioengineering Systems, where he has been an assistant professor, an associate professor, and a professor. He defended his candidate of technical science thesis in 1971 and his doctor of technical science thesis in 1990. Currently he is a department chairman at the Kharkov Aviation Institute. His research areas are multifrequency oscillators and multichannel radar imaging systems.

Heikki Huttunen received his MSc in mathematics from the University of Tampere, Finland, in 1995. He is currently starting work toward a doctoral degree at Tampere University of Technology while working on a digital signal processing project. His research interests include optimization methods, e.g., genetic algorithms, in optimization of nonlinear digital filters. He has also been studying applications of digital signal processing in the security industry.

Jaakko T. Astola received BSc, MSc, Licentiate, and PhD degrees in mathematics from Turku University, Finland, in 1972, 1973, 1975, and 1978, respectively. From 1976 to 1977 he was a research assistant with the Research Institute for Mathematical Sciences, Kyoto University, Japan. Between 1979 and 1987 he was with the Department of Information Technology, Lappeenranta University of Technology, Lappeenranta, Finland, holding various teaching positions in mathematics, applied mathematics, and computer science. From 1988 to 1993 he was an associate professor of applied mathematics at Tampere University, Finland. Currently, he is a professor of digital signal processing at Tampere University of Technology. His research interests include image and signal processing, coding theory, and statistics.